Journal of Materials Science: Materials in Electronics
https://doi.org/10.1007/s10854-019-02155-6

Dielectric behavior in erbium-doped tellurite glass for potential high-energy capacitor

M. N. Azlan[1] · S. Z. Shafinas[2] · M. K. Halimah[2] · A. B. Suriani[1]

Received: 20 March 2019 / Accepted: 4 September 2019

Abstract
The use of erbium ions, Er^{3+} to enhance the dielectric properties is investigated in tellurite glass system for the first time, to the best of our knowledge. A glass series of tellurite glass with chemical composition, $\{[(TeO_2)_{70}(B_2O_3)_{30}]_{70}(ZnO)_{30}\}_{100-y}(Er_2O_3)_y$ (y = 0, 0.005, 0.01, 0.02, 0.03, 0.04 and 0.05) was fabricated via melt-quenched technique. The X-ray diffraction and Fourier transform infrared spectroscopy analysis proved the amorphous structure and the formation of nonbridging oxygen in the glass system. The Er^{3+} ions affect greatly to the dielectric constant, ε′ in which the dielectric constant, ε′ show high value at a lower frequency and higher temperature (above 110 °C). The reduction of dielectric constant, ε′ is found with the increment value of frequency, which corresponds to the formation of the hindrance effect on heavy dipoles caused by the mixed transition-ion effect. Meanwhile, the dielectric constant, ε′ is enhanced with the increase of temperature. The activation energy of the glass system is found to decrease, which is due to the high polarizability of Er^{3+} ions in the glass system. Based on these results, the erbium-doped tellurite glass is a potential kind of high-energy capacitor.

1 Introduction

Extensive research on high energy density storage capacitors had been done to achieve high dielectric constant and high breakdown strength (> 5 MV/cm) [1]. Polymers and ceramics are the most common materials to be used for such applications due to their high breakdown strength (> 5 MV/cm) [1]. However, these materials have relatively low dielectric constant ε′, which reduce their capabilities in the high-energy capacitor. Tellurite glass is known to have large dielectric constant ε′ and high breakdown strength, which is highly beneficial for high-energy capacitor [2]. The high compatibility of host glass with rare-earth ions is crucial to increase the polarizability of the glass system, which in turn increase the activation energy. Tellurite glass has the highest compatibility with various kind of rare-earth oxide as compared with heavy metal glasses [3]. Moreover, tellurite glass has high electrical conductivity, which is due to the unshared pair of electrons of TeO_4. Based on these properties, tellurite glass has a high potential for the high-energy capacitor.

Tellurite glass is not stable to form on their own. Thus, the glass modifiers are essential to stabilize the glass formation. Zinc oxide is useful to reduce the melting temperature and have high polarizability, which is necessary to enhance the dielectric properties. Meanwhile, boron oxide has a unique characteristic, which is the ability to convert the coordination number with oxygen and easily to form various structural units. Furthermore, borate oxide has high mechanical properties and increase the amount of nonbridging oxygen in the glass network. Hence, the combination of zinc oxide, ZnO, and borate oxide, B_2O_3 in the glass network may enhance the stability and strength of the tellurite glass network.

To achieve high-energy capacitor, a glass material with a high dielectric constant is necessary. The dielectric properties of tellurite glass depend on the type of modifiers exists in the glass network and their field strength. The presence of high polarizability of modifiers reduce the dielectric loss and enhance the dielectric constant in the tellurite glass system. Generally, the dielectric properties of tellurite glass can be altered by doping rare-earth oxide in the glass network [4]. Erbium ions, Er^{3+} are known to have high coordination number and polarizability, which may enhance the dielectric properties and reduce the dielectric loss. Previous research

✉ M. N. Azlan
azlanmn@fsmt.upsi.edu.my

[1] Physics Department, Faculty of Science and Mathematics, Universiti Pendidikan Sultan Idris, 35900 Tanjung Malim, Perak, Malaysia

[2] Physics Department, Faculty of Science, University Putra Malaysia, 43400 UPM Serdang, Selangor, Malaysia

Published online: 07 September 2019

by Sajna et al. found that the dielectric properties of tellurite glass can be tuned by altering the concentration of erbium oxide [5]. Xu et al. found that the rare earth oxide has a major role in reducing the dielectric loss in tellurite glass by increasing the concentration of rare earth oxide [6]. Moreover, there are only a few studies up to date on the role of Er^{3+} to improve the dielectric properties of tellurite glass system. Hence, the research on the erbium oxide effect on dielectric properties of tellurite glass system is the first step to produce high-energy capacitor.

Many works have been done to enhance the dielectric constant such as using the ceramics for the primary materials of the capacitor, the mixed alkali effect, and stabilizing the network structure [1, 7]. However, only a few efforts had been made to utilize the tellurite glass doped with rare-earth oxide to be used in the capacitor. It is known that glass materials have unique properties to enhance the dielectric properties such as the high number of non-bridging oxygen and great compatibility with rare earth oxide [8]. It is highly necessary to investigate the capability of tellurite glass to be used in the high-energy capacitor. The present work is aimed to measure and analyze both temperature and frequency dependencies of the dielectric constant and dielectric loss for the application of high-energy capacitor.

2 Experimental

The raw materials of tellurium(IV) oxide, TeO_2 (99.99%, Puartronic, Alfa Aesar), boron oxide, B_2O_3 (99.98%, Assay, Alfa Aesar), ZnO (99.99%, Assay, Alfa Aesar) and erbium(III) oxide, Er_2O_3 (99.9%, Reacton, Alfa Aesar) were used to synthesize the glass materials. The chemical composition of the tellurite glass doped with different concentrations of erbium oxide, Er_2O_3 is as follows $\{[(TeO_2)_{70}(B_2O_3)_{30}]_{70}(ZnO)_{30}\}_{100-y}(Er_2O_3)_y$ where y = 0, 0.005, 0.01, 0.02, 0.03, 0.04, 0.05)}. The glass samples were prepared via the melt-quenched technique. The raw materials were weighed and mixed thoroughly. The batches were placed in an alumina crucible and preheated in an electrical furnace at temperature 400 °C for 30 min to reduce any tendency towards volatilization. The alumina crucible was transferred to a second furnace for the melting process at 900 °C for 2 h. The molten was then poured in stainless steel cylindrical-shaped split mold which had been preheated at 350 °C for 30 min. The mold containing the glass sample was annealed at 400 °C for 1 h. The furnace was turned off and allowed to cool down at room temperature for 24 h. The prepared glass sample was free from bubbles and pink in color. The sample was cut and polished into pallet with a thickness of 2 mm. The samples were ground into powder form for X-ray diffraction (XRD) and Fourier transform infrared spectroscopy (FTIR) measurement. The density of the samples was determined by the Archimedes principle, and the molar volumes were calculated. The glassy state of the system was characterized by using XRD measurement (X'pert Pro PanAlytical). The IR spectra were recorded using FTIR in the frequency range of 280–4000 cm^{-1} at room temperature. The dielectric constant and dielectric loss were characterized in the temperature range of 50–200 °C at frequency range 10^{-2}–10^6 Hz by using high dielectric resolution analyzer (Novo-Control).

3 Results and discussion

3.1 Density and molar volume

Figure 1 illustrates the density and molar volume of erbium-doped tellurite glass. It can be seen from Fig. 1 that the density is increased from 3.630 to 3.960 g/cm^3 along with erbium oxide concentration. The increment in the density can be explained by comparing the density of Er_2O_3 with TeO_2. It is obvious that the density of Er_2O_3 (8640 kg/m^3) is higher than TeO_2 (5670 kg/m^3), which cause the density to increase. The change in density corresponds to the change in the atomic mass and atomic volume of constituent elements. It is known that the atomic weight of erbium oxide is 167.259 g/mol which is heavier than the atomic mass of ZnO (81.408 g/mol), B_2O_3 (69.620 g/mol) and TeO_2 (159.608 g/mol). The high in atomic weight of erbium oxide may contribute to the increase in density.

Erbium oxide is known to have trivalent cation Er^{3+} which tends to release three electrons. Each of the Er^{3+} ions has a high tendency to capture one electron from the oxygen and thus, breaks the continuous network chain. The breaking of the continuous network leads to the formation of non-bridging oxygen. Each of the Er^{3+} ions is capable of producing three non-bridging oxygen ions, which increase the number of non-bridging oxygen in the glass network. The high number of non-bridging oxygen in the glass network may increase the density of the glass system. The degree of crosslinking in those glasses is progressively degraded, which leads to an increase in density. Hence, the increase in density may be due to the change in coordination number, crosslink density, and dimensional interstitial space and structural compactness [9, 10]. It can be summarized that the introduction of Er^{3+} ions which have a high number of charges and coordination number may lead to the formation of new linkages in the glass structure.

Molar volumes are found to increase with an increase of erbium concentration but slightly decrease at 0.04 mol of erbium. The behavior of molar volume follows an opposite trend, but, in this study, it is found that the density and the molar volume increase along with erbium oxide concentration. The increase in molar volume is due to the atomic

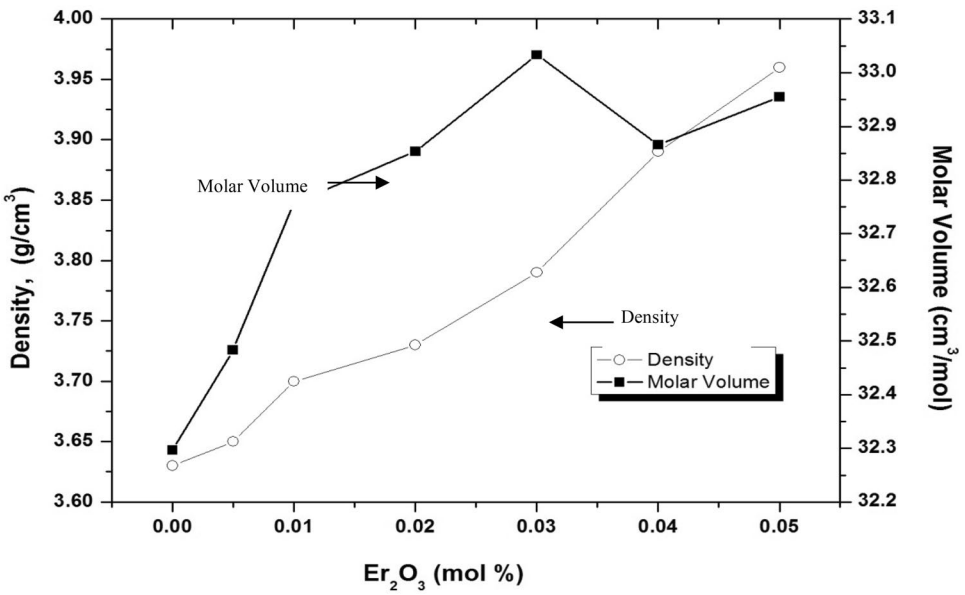

Fig. 1 Variation of the mole fraction of Er_2O_3 with density and molar volume of erbium doped tellurite glass

radius of Er^{3+} (1.78 Å), which is higher than that of tellurite (1.60 Å). Besides, the increase of non-bridging oxygen may also contribute to the increase in molar volume. The transformation of trigonal pyramidal [TeO_3] structural unit to trigonal bipyramidal [TeO_4] unit indicates the high density of non-bridging oxygen. The slight decrease of molar volume at 0.04 mol may be due to the rearrangement of the lattice and compact structure in the glass network [11]. Another possibility is that the decrease in bond length between the atoms may increase the stretching force constant of the bonds in the glass network. Hence, the increase in stretching force constant may result in more compact and denser glass [11].

It is known that the borate oxide, B_2O_3 consists of threefold coordinated with oxygen when upon modification with a rare earth oxide. The oxygen is lost by the oxide dissociation and will result in a transformation of BO_4 coordination into BO_3 coordination [12]. Thus, the increase in BO_3 unit leads to a rise in non-bridging oxygen and responsible for the decrease in molar volume at 0.04 mol. The creation of non-bridging oxygen will increase the distance between structural groups of the studied glasses system. The larger the values of ionic radii between the molecules may increase the overall molar volume of the glass system. Another possibility is that the increase in molar volume may be due to the molar volume of tellurite glass 31.29 cm^3, which is greater than tellurite crystal 26.60 cm^3. Hence, the difference in molar volume between tellurite glass and tellurite crystal correlates with the longer number of TeO_2 units that can be accommodated in the more open structure of the vitreous state.

3.2 Fourier transform infrared (FTIR)

Figure 2 represents the FTIR spectra of erbium-doped tellurite glass. The peaks positions and their assignments are shown in Table 1. The assignment of pure tellurite oxide, TeO_2 is centered at 640 cm^{-1} [13, 14]. The tellurite oxide, TeO_2 structural unit is converted to trigonal pyramid TeO_3 and bipyramid TeO_4 after the glass formation. The absorption band found in the range of 650–700 cm^{-1} correlates with TeO_3 group, and the absorption band in the range of 600–650 cm^{-1} correspond to TeO_4 group. It can be seen from the figure. that the absorption band at 656–664 cm^{-1} is observed which proved the assignment of trigonal pyramid TeO_3 group. This assignment is the indication of the existence of non-bridging oxygen in the glass system.

The non-existence of tellurite oxide, TeO_2 assignment in FTIR spectra shows that the bridging oxygen of tellurite oxide, TeO_2 is completely converted to non-bridging oxygen. The inclusion of zinc oxide, ZnO in the glass system introduces the formation of Te–O–Zn by breaking up the Te–O–Te bond at a low proportion of zinc oxide, ZnO and the Te–O–B bonds indicates the coordination effects called as dangling bonds (Te-0- .. Zn^{2+}.. O–Te), which in turn decreased TeO_3 units by forming TeO_4 units [15]. The appearance of the absorption peak at 414 cm^{-1} and 421 cm^{-1} of tellurite glass system with 0 mol of erbium indicates that the zinc oxide, ZnO participate in the glass network with ZnO_4 structural units and alternate with TeO_4 units. Besides that, this band disappears when Er_2O_3 content is introduced into the glass network. This trend

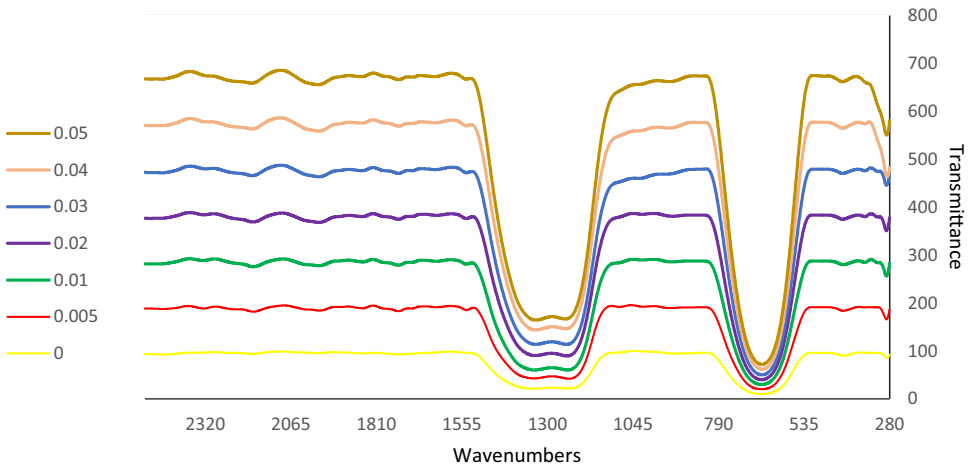

Fig. 2 FTIR spectra of erbium doped tellurite glass

Table 1 Assignment of infrared transmission bands of sample glass

No.	0.005	0.01	0.02	0.03	0.04	0.05	Assignments
1	1340	1331	1325	1327	1333	1339	Trigonal B–O bond stretching vibrations in isolated trigonal BO_3 units [1, 2]
2	1233	1257	1248	1243	1246	1251	Trigonal B–O bond stretching vibrations in isolated trigonal BO_3 units from boroxyl groups [1, 2]
3	660	661	660	656	658	663	TeO_3 group are exists in all tellurite containing glass [1, 2]
4	–	–	–	–	421	–	ZnO participate in the glass network with ZnO_4 structural units and alternate TeO_4 units [1, 2]

indicates that the zinc lattice is completely broken down after the inclusion of erbium oxide.

The pure borate oxide, B_2O_3 consists of a random network of boroxyl rings at around 806 cm^{-1} where this band disappear during the formation of the glass network. The BO_3 and BO_4 groups were introduced after the glass formation, and these groups were in the form of a random network [16]. The assignment of IR bands to specific vibrations in borate groups will be based on the work of Krogh–Moe [16]. The transmission spectra of borate glass can be divided into three regions: (1) 600–800 cm^{-1} (bending vibrations of various borate arrangement B–O–B), (2) 800–1200 cm^{-1} (B–O stretching of tetrahedral BO_4^- units), (3) 1200–1800 cm^{-1} (B–O stretching of trigonal BO_3 units). The band at about 1233–1253 cm^{-1} associated with the B–O (B) stretching vibrations of polymerized BO_3 groups [17]. The absorption band in the range 1327–1343 cm^{-1} correspond to the trigonal B–O bond stretching vibrations in isolated trigonal BO_3 units.

Furthermore, the absorption band in the range 1200–1253 cm^{-1} are assigned to the trigonal B–O bond stretching vibrations of BO_3 units from boroxyl groups and the absorption band in the range 1388–1410 cm^{-1} correspond to trigonal B–O bond stretching vibrations of BO_3 units from varied types of borate groups. These bands can be from the FTIR spectra in the range of 1233–1253 cm^{-1} and 1327–1343 cm^{-1}. The increase of erbium oxide concentrations leads to broaden the absorption band and reduce the intensity [18]. In general, the shift of the absorption band depends on the changes in the composition of the glass network.

3.3 X-ray diffraction (XRD)

The XRD analysis was used to confirm the amorphous or crystalline state of the materials. The XRD spectra of erbium doped tellurite glass are shown in Fig. 3. As can be seen from the figure, the broad peaks at lower scattering angles are found at around $2\theta = 30°$ indicating the amorphous structural arrangement. The sharp peaks indicating the crystal structural are absent which prove that the glass system is completely amorphous. In general, a glass is supposed to be a random arrangement of molecules and below the transformation region, the molecules are much less mobile.

3.4 Electrical properties

3.4.1 Frequency dependence of the dielectric properties

The plot of dielectric constant (ε') along with the frequency at various temperature is shown in Fig. 4. It can be seen from the figure that the dielectric constant, ε' decreases with an increase of frequency which is due to the dielectric dispersion from the lag of the polarization process of the glass molecules [19]. This trend is in accordance with the previous research, which found a decrease in dielectric

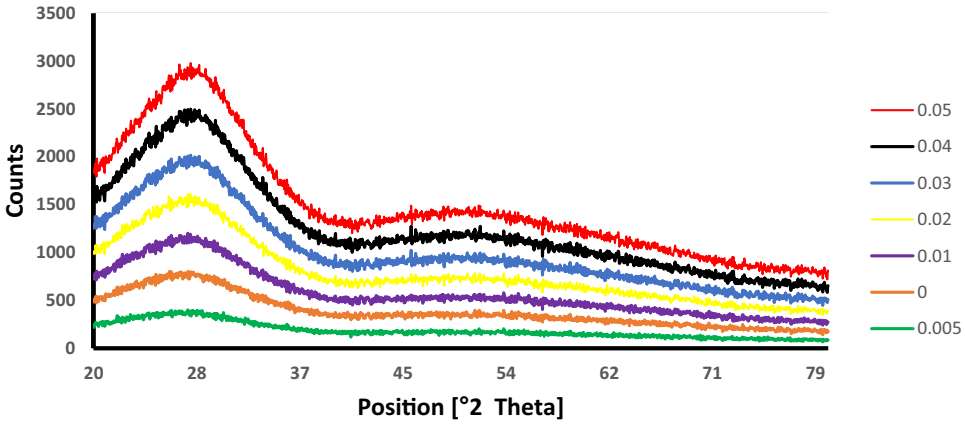

Fig. 3 X-ray diffraction pattern of erbium doped tellurite glass

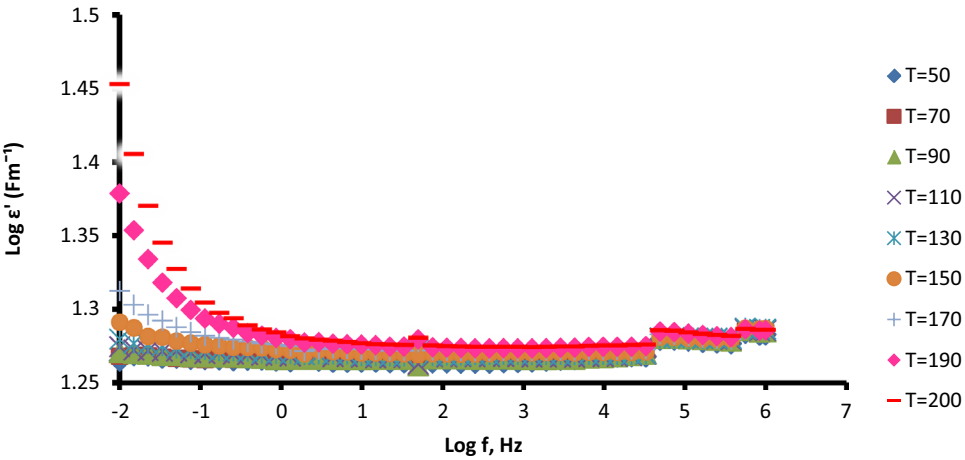

Fig. 4 Graph log dielectric constant versus log frequency of erbium doped tellurite glass at different temperature

constant with an increase of frequency [20]. The frequency dependent of dielectric constant is found in tellurite glass system. The polarization of glass is due to the vibrational configuration group. Meanwhile, the lattice defects is due to the deformation of the oxygen around tellurite and the boron ions. At low frequency, the dielectric constant increases with temperature, which is typical in oxide glasses and is not an indication for spontaneous polarization.

The features of the dielectric can be explained by considering the factor of frequencies, ionic, dipolar and interfacial polarization. In fact, all type of polarization contributes to the dielectric constant. The variation of dielectric constant, ε' along with frequency is highly related to the polarization of ions from the applied field [21]. The contributions of interfacial polarization occur at frequency below 100 Hz. The interfacial polarization is due to the ionic motion in the presence of an electric field. At low frequency (below 100 Hz), the impurity ion diffuse under the influence of the reversal applied field with the alternating voltage. According to the previous work [13], erbium ions, Er^{3+} possess cation polarizability equal to 2.253 A^3 which higher than tellurite (1.595 A^3), zinc (0.283 A^3) and borate (0.002 A^3). Based on these features, it can be assumed that the erbium ions, Er^{3+} are easier to polarize due to trivalent Er^{3+} ions and possess high polarity. Meanwhile, the nonbridging oxygen in the glass system possesses a high number of free electrons. Hence, the formation of nonbridging oxygen will increase the polarization mechanism.

As the polarization increases, the dielectric constant will be increased. Moreover, the increase in frequency leads to the restriction of electron hopping from the dielectric field fluctuations and hence, reduce the number of dielectric constant, ε' [22]. Besides that, the ionic motions are sensitive to the frequency of the alternating field and limit the mobility of the ionic motions at a higher frequency. From Fig. 4, it can be seen that the dielectric constant is approaching constant after 1 kHz, which is due to the decreasing number of dipoles.

The frequency dependence of dielectric loss, ε'' is shown in Fig. 5. The change in dielectric loss strongly depends on the thermally activated relaxation of free rotating dipoles. The thermal energy is the only type of relaxation loss at higher temperatures, which is due to the electrical conduction with electrons hopping [23].

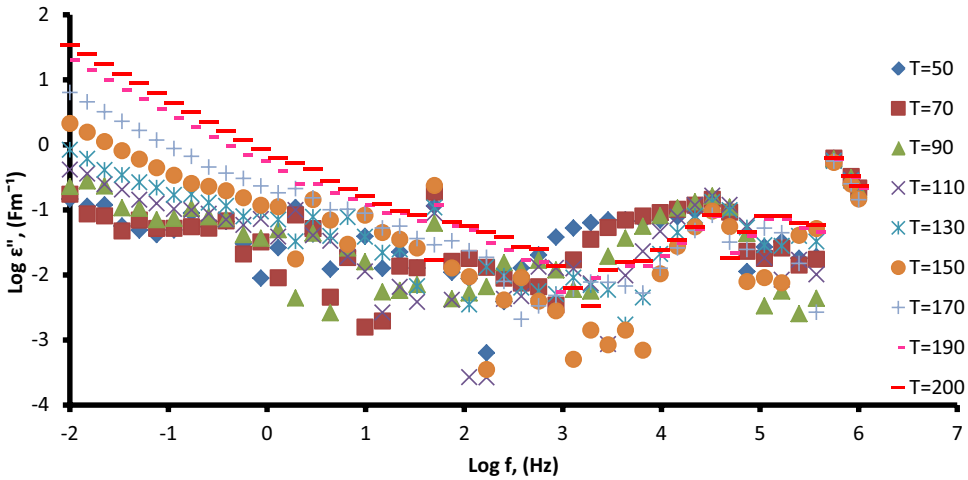

Fig. 5 Graph log dielectric loss factor versus log frequency of erbium doped tellurite glass at different temperature

The variation of dielectric loss ε″, is observed clearly in the figure as the dielectric loss, ε″ is decreased with increase in frequency. Meanwhile, the dielectric loss is found to increase with an increase in temperature. It can be observed that there is a small broad dielectric loss absorption at a certain frequency and shifted towards the higher frequency with an rise in temperature.

The dielectric loss ε″, decreases monotonously with an increase of frequency and reach a minimum value at high frequency, which is due to the migration of ions. The similar trend is found by Mohamed et al. which proposed a decrease in dielectric loss ε″, with an increase of frequency in tellurite glass [20]. The migration ions are the primary source of dielectric loss at lower frequencies [24]. At high frequency, the vibration of the electrons may be the only source of dielectric loss. Besides, the appearance of dielectric loss at high frequency, may due to the energy degenerated from the movement and vibration of free charge and the dipole polarization in the glass network. The dielectric loss ε″ decreases to a lower value at 1 MHz, which is strongly due to the vibrations of ions.

3.4.2 Temperature dependence of the dielectric properties

Figures 6 and 7 show the variation of dielectric constant (ε') and dielectric loss factor (ε'') in the range 50–200 °C of temperature with 100 Hz of frequency, respectively. In Fig. 6, it can be seen that the dielectric constant, ε' increases with an increase in temperature and increases more rapidly at high temperature. This behavior is typical to the polar dielectrics in which the orientation of dipoles is facilitated with the rising of temperature, and thereby, the dielectric constant is increased. Moreover, the increase in the dielectric constant with temperature indicates the increase of orientation polarization of the lattice defects, polar portions in the amorphous phase and the rise in the number of translational motion of the free charges. These phenomena occur due to the formations of nonbridging oxygen in the glass system.

At low temperature, the effect of electronic and ionic components to the polarizability is small. Furthermore, the increase of dielectric constant, ε' with temperature is usually associated with a decrease in bond energies [25]. As the temperature increases, two types of effects on the dipolar polarization may occur. First, the weakening of the intermolecular

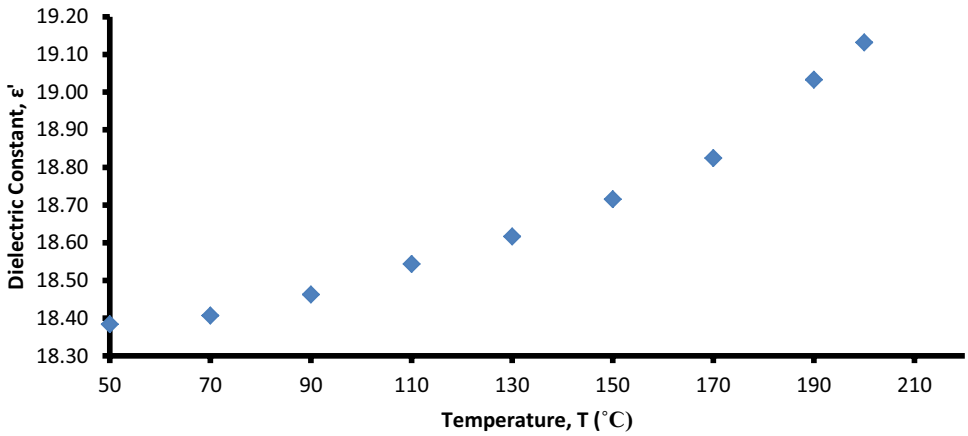

Fig. 6 Graph dielectric constant versus temperature of erbium doped tellurite glass at frequency 100 Hz

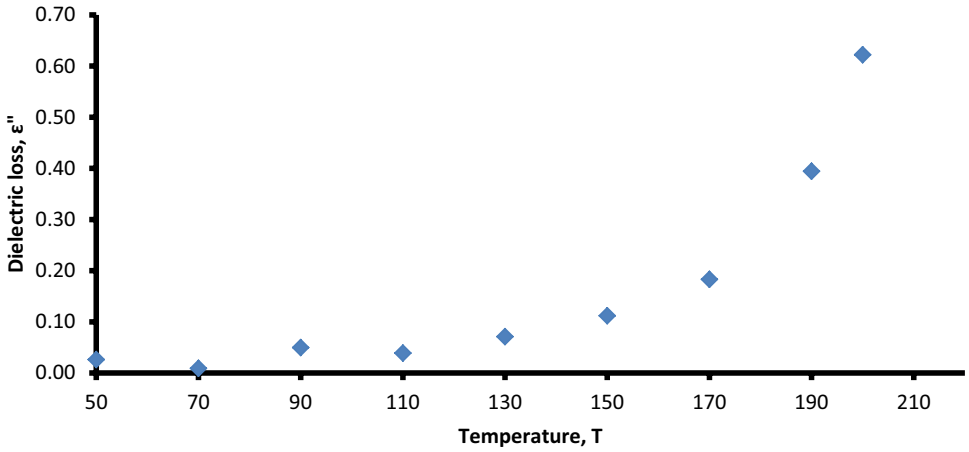

Fig. 7 Graph dielectric loss versus temperature of erbium doped tellurite glass at frequency 100 Hz

forces and result in the enhancement of the orientational vibration. Second, the increase of the thermal agitation and leads to the strong disturbance of the orientational vibrations [26]. As the temperature is increased, the electronic and ionic polarizability sources start to increase [27]. This trend might be due to the fact that as the frequency increases, the polarizability from ionic and orientation sources decreases and finally disappears due to the inertia of the ions. The obtained value of the dielectric constant is higher than the previously reported data in tellurite glass by Hisam et al. which found that the dielectric constant value is in the range of 1.0–4.5 [18].

In addition, it can be seen from the Fig. 7 that the dielectric loss increases with an increase in temperature, which may be attributed to the relaxation loss at low temperature. As the temperature increases, there is a reduction in the relaxation loss and results in the rise in conduction loss more rapidly. From Fig. 7, it can be observed that the dielectric loss, ε″ is increased rapidly at high temperature (above 150 °C) and low-frequency, which is strongly due to the space charge polarization. The space charge polarization can be explained by using the Shockley–Read mechanism for low and middle-order frequencies and at high temperature.

3.4.3 Fitting models of the dielectric properties

Figure 8 illustrates the graph of dielectric constant, ε' and dielectric loss, ε'' along with frequency. It can be seen from the figure that the two processes are present, which is at low and high-frequency dispersion. The spectra parameters can be plotted by using the standard models, such as Debye, Cole–Cole, Cole–Davidson, Havriliak Nagami, Dissador Hill, and the dc and quasi-dc. The spectral function can be expressed as:

$$C^*(\omega) = C_1^* + C_0\omega^m,$$

$$C^*(\omega) = \frac{C_0 C_b (i\omega)^{m-1}}{C_0 + C_b(i\omega)^{m-1}} + C_a(\omega)^m,$$

where m and n are constant for a given material. The analysis of data assumes that the impedance can be represented by

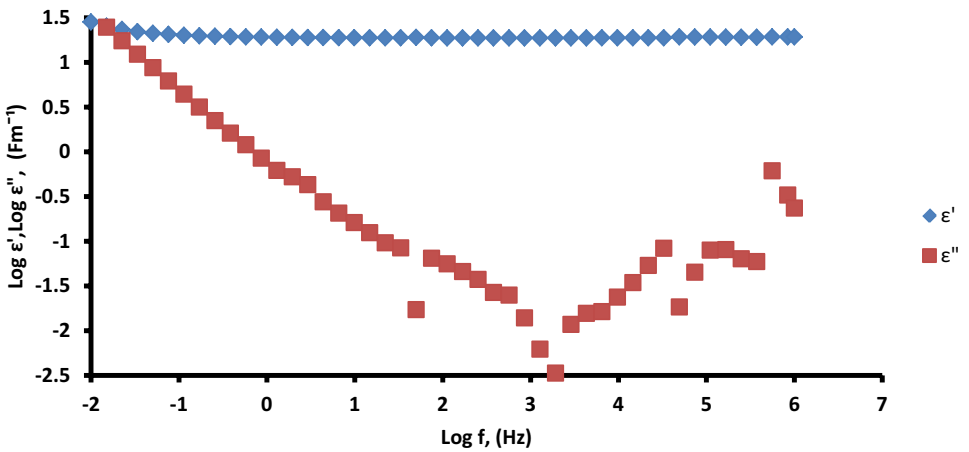

Fig. 8 Graph dielectric constant and dielectric loss versus frequency of erbium doped tellurite glass at frequency 200 Hz

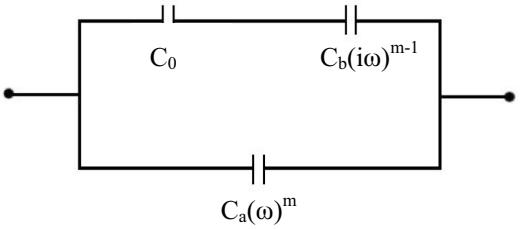

Fig. 9 Equivalent circuit of erbium doped tellurite glass at 200 °C

a circuit shown in Fig. 9. The illustrated dielectric spectrum and the fitting of the 0.03 mol of erbium oxide at 200 are shown in Fig. 10. It can be seen from the figure that the theoretical values are in good agreement with experimental ones.

3.4.4 Activation energy, E_a

The activation energy, E_a is obtained from the correlated master curve in all range of frequency and temperature, as illustrated in Fig. 11. The master curve technique consists of the translation of dielectric data with various temperatures. The plots of dielectric constant and dielectric loss seem to be merged in such a way that the overall shape of the resultant

Fig. 10 Plot of experimental and theoretical value of erbium doped tellurite glass at 200 °C

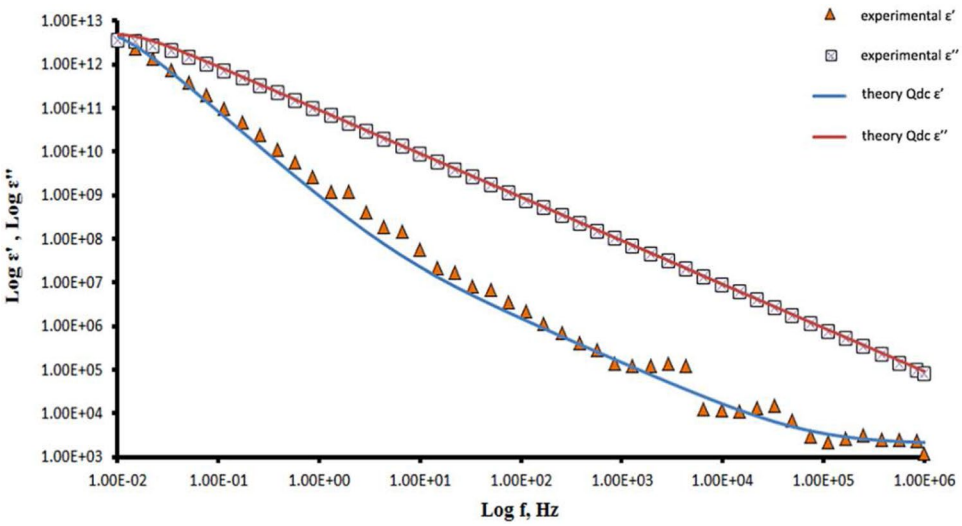

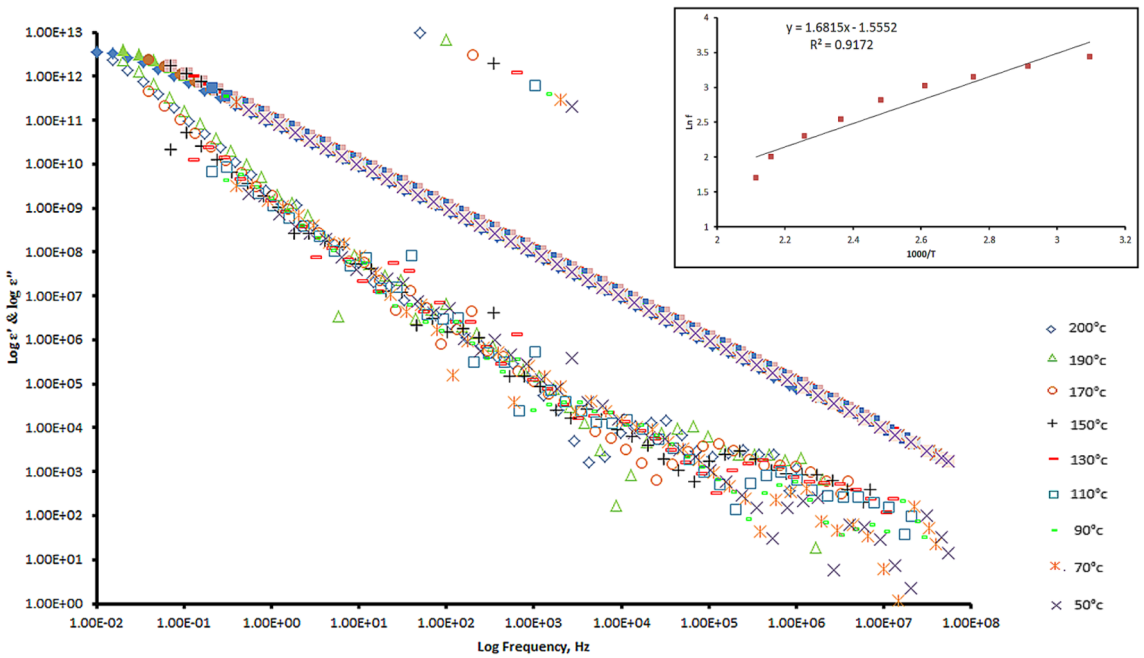

Fig. 11 Plot of experimental and theoretical value of erbium doped tellurite glass at 200 °C

does not change with temperature. The plot of Ln f against 1000/T (K^{-1}) is represented in Fig. 11 and yielded a straight line which was fitted by using the Arrhenius equation from the following expression:

$$f = f_0 \exp\left(+\frac{E_a}{kT}\right),$$

where f_0 and E_a are the reference frequency and activation energy, respectively. The activation energy, E_a is determined from the slope, and the parameter k is the Boltzmann constant. The E_a was plotted in Fig. 12 and tabulated in Table 2. It is found that the activation energy value decreases from 0.1389 to 0.0863 eV along with erbium oxide content. Previous research reported that the energy band gap is linearly decreased with an increase of erbium oxide content [11]. The decrease in the bandgap is strongly due to the decrease in activation energy. Hence, the trend of activation energy, E_a is in accordance with the value of optical band gap from the previous research. The oxygen ions in the glass system are the most polarizable ion and construct more space charge polarization in the glass network. These features lead to an increase of the dielectric parameters as observed and the decrease in activation energy (eV) [11].

Table 2 Activation energy of erbium doped tellurite glass

Sample	Activation energy (eV)
0	0.1389
0.01	0.1397
0.03	0.1180
0.04	0.1061
0.05	0.0863

4 Conclusions

The XRD analysis confirmed that the glass samples are in an amorphous structure. The FTIR analysis consists of several bands, which indicates the characteristic of Te–O and B–O vibrational groups. The density of the prepared glass samples was found increases with an increase of erbium oxide. This trend was due to the high value of the atomic weight of erbium oxide as compared with tellurite oxide and the formation of non-bridging oxygen. The molar volume was found increases with an increase of erbium oxide. This trend was due to the large value of ionic radii of erbium oxide as compared to the other oxides in this glass system. The dielectric properties (dielectric constant, ε', and dielectric loss factor, ε'') of erbium-doped tellurite glass system decreases with a rise in frequency but increases with an increase of temperature. Such trend was found due to the electron polarization and space charge accumulation at the glass–electrode interface. The fitting model using equation $C^*(\omega) = \frac{C_0 C_b (i\omega)^{m-1}}{C_0 + C_b (i\omega)^{m-1}} + C_a(\omega)^m$ was proposed. The activation energy (E_a) was found to decrease along with erbium oxide concentration which is mainly due to to the increase of the bond length of BO_3 structural unit which was the most polarizable ions and constructs more space charge polarization within the glass network. Hence, based on these results, we have managed to obtain potential materials to be used in the high-energy capacitor with excellent dielectric properties.

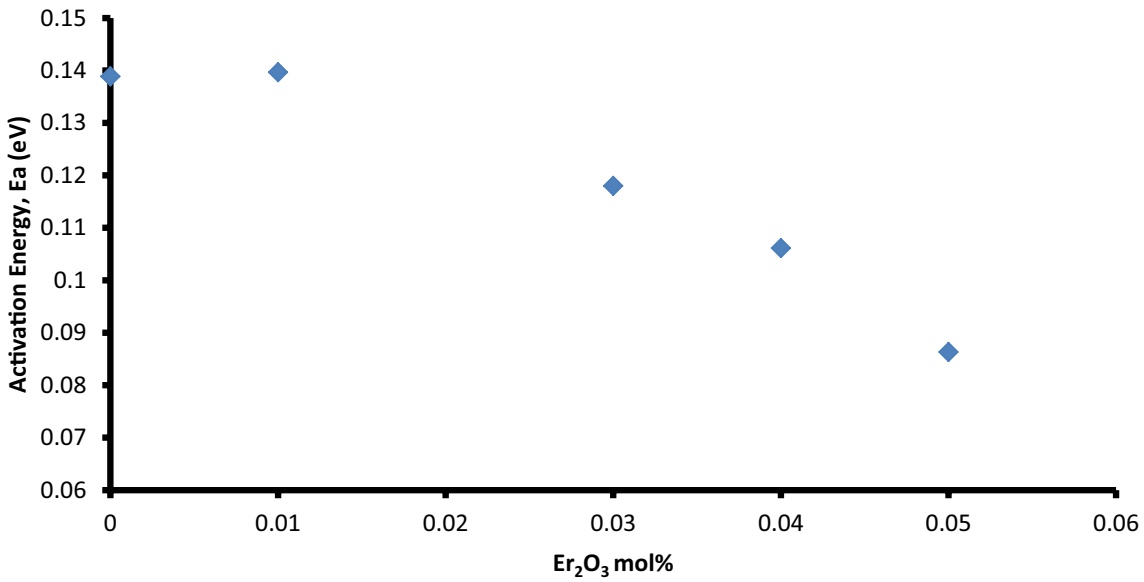

Fig. 12 Activation energy of erbium doped tellurite glass

Acknowledgements The writers appreciate the financial support for the work from the Ministry of Higher Education of Malaysia and Universiti Pendidikan Sultan Idris through Skim Geran Penyelidikan Fundamental, FRGS [Code 2019-0006-102-02 (FRGS/1/2018/STG07/UPSI/02/1)] and Geran Penyelidikan Universiti, GPU (Code 2018-0139-103-1). The authors would like to thank the following institutions for equipment support: Faculty of Science and Mathematics, Universiti Pendidikan Sultan Idris and Faculty of Science, Universiti Putra Malaysia.

References

1. V. Fuertes, M.J. Cabrera, J. Seores, D. Muñoz, J.F. Fernández, E. Enríquez, Microstructural study of dielectric breakdown in glass–ceramics insulators. J. Eur. Ceram. Soc. **39**, 376–383 (2019)
2. M.N. Azlan, M.K. Halimah, Role of Nd^{3+} nanoparticles on enhanced optical efficiency in borotellurite glass for optical fiber. Results Phys. **11**, 58–64 (2018)
3. N.N. Yusof, S.K. Ghoshal, M.N. Azlan, Optical properties of titania nanoparticles embedded Er^{3+} doped tellurite glass: Judd-Ofelt analysis. J. Alloy Compd. **724**, 1083–1092 (2017)
4. M.K. Halimah, M.F. Faznny, M.N. Azlan, H.A.A. Sidek, Optical basicity and electronic polarizability of zinc borotellurite glass doped La^{3+} ions. Results Phys. **7**, 581–589 (2017)
5. M.S. Sajna, S. Thomas, C. Jayakrishnan, C. Joseph, P.R. Biju, N.V. Unnikrishnan, NIR emission studies and dielectric properties of Er^{3+}-doped multicomponent tellurite glasses. Spectrochim. Acta A **161**, 130–137 (2016)
6. K.L. Xu, Y. Yan, L. Zhang, H.L. Pan, J.F. Zhao, X. Jia, G. Wang, H.T. Wu, Study on structural, dielectric, thermal and chemical characteristics of aluminoborosilicate glasses doped by rare earth oxides. Mater. Technol. **29**, A40–A43 (2014)
7. D. Jiang, J. Chen, B. Lu, J. Xi, F. Shang, J. Xu, G. Chen, Preparation, crystallization kinetics and microwave dielectric properties of CaO–ZnO–B_2O_3–P_2O_5–TiO_2 glass–ceramics. Ceram. Int. **45**(7, Part A), 8233–8237 (2019)
8. P.-K. Fischer, G.A. Schneider, Dielectric breakdown toughness from filament induced dielectric breakdown in borosilicate glass. J. Eur. Ceram. Soc. **38**, 4476–4482 (2018)
9. S. Zheng, Y. Zhou, D. Yin, X. Xu, Y. Qi, S. Peng, The 1.53 μm spectroscopic properties and thermal stability in Er^{3+}/Ce^{3+} codoped TeO_2–WO_3–Na_2O–Nb_2O_5 glasses. J. Quant. Spectrosc. Radiat. Transf. **120**, 44–51 (2013)
10. N. Yaru, L. Chunhua, Z. Yan, Z. Qitu, X. Zhongzi, Study on optical properties and structure of Sm_2O_3 doped boron-aluminosilicate glass. J. Rare Earths **25**, 94–98 (2007)
11. A.M. Noorazlan, H.M. Kamari, S.S. Zulkefly, D.W. Mohamad, Effect of erbium nanoparticles on optical properties of zinc borotellurite glass system. J. Nanomater. (2013). https://doi.org/10.1155/2013/940917
12. C. Eevon, M.K. Halimah, A. Zakaria, C.A.C. Azurahanim, M.N. Azlan, M.F. Faznny, Linear and nonlinear optical properties of Gd^{3+} doped zinc borotellurite glasses for all-optical switching applications. Results Phys. **6**, 761–766 (2016)
13. M.H. Shaaban, A.A. Ali, M.K. El-Nimr, The AC conductivity of tellurite glasses doped with Ho_2O_3. Mater. Chem. Phys. **96**, 433–438 (2006)
14. P. Gayathri Pavani, K. Sadhana, V. Chandra Mouli, Optical, physical and structural studies of boro zinc tellurite glasses. Physica B **406**, 1242–1247 (2011)
15. Y.B. Saddeek, E.R. Shaaban, E.S. Moustafa, H.M. Moustafa, Spectroscopic properties, electronic polarizability, and optical basicity of Bi_2O_3–Li_2O–B_2O_3 glasses. Physica B **403**, 2399–2407 (2008)
16. S.N. Nazrin, M.K. Halimah, F.D. Muhammad, J.S. Yip, L. Hasnimulyati, M.F. Faznny, M.A. Hazlin, I. Zaitizila, The effect of erbium oxide in physical and structural properties of zinc tellurite glass system. J. Noncryst. Solids **490**, 35–43 (2018)
17. X.A. Shen, T.F. Xu, X.D. Zhang, S.X. Dai, Q.H. Nie, X.H. Zhang, Effect of SiO_2 content on the thermal stability and spectroscopic properties of Er^{3+}/Yb^{3+} co-doped tellurite borate glasses. Physica B **389**(2), 242–247 (2007)
18. R. Hisam, A.K. Yahya, H. Mohamed Kamari, Z.A. Talib, R.H. Yahaya Subban, Anomalous dielectric constant and AC conductivity in mixed transition-metal-ion xFe2O3–(20–x)MnO2–80TeO2 glass system. Mater. Express **6**(2), 149–160 (2016)
19. M. Bosca, L. Pop, G. Borodi, P. Pascuta, E. Culea, XRD and FTIR structural investigations of erbium doped bismuth–lead–silver glasses and glass ceramics. J. Alloys Compd. **479**, 579–582 (2009)
20. E.A. Mohamed, M.G. Moustafa, I. Kashif, Microstructure, thermal, optical and dielectric properties of new glass nanocomposites of $SrTiO_3$ nanoparticles/clusters in tellurite glass matrix. J. Noncryst. Solids **482**, 223–229 (2018)
21. P.N. Musfir, S. Mathew, V.P.N. Nampoori, S. Thomas, Investigations on frequency and temperature dependence of AC conductivity and dielectric parameters in $Ge_{20}Ga_5Sb_{10}S_{65}$ quaternary chalcogenide glass. Optik **182**, 1244–1251 (2019)
22. R. Hisam, A.K. Hayati Yahya, D. Said, M.F. Mustafa, AC conductivity and dielectric properties of strontium–lead borate glasses. Int. J. Eng. Technol. (UAE) **7**, 143–146 (2018)
23. D. He, C. Gao, Effect of boron on crystallization, microstructure and dielectric properties of CBS glass–ceramics. Ceram. Int. **44**, 16246–16255 (2018)
24. P. Tripathi, P. Kumari, V.K. Mishra, R. Singh, S.P. Singh, D. Kumar, Effect of PbO–B_2O_3–BaO–SiO_2 glass additive on dielectric properties of $Ba_{0.5}Sr_{0.5}TiO_3$ ceramics for radio-frequency applications. J. Phys. Chem. Solids **127**, 60–67 (2019)
25. S. Wang, J. Tian, T. Jiang, J. Zhai, B. Shen, Effect of phase structures on dielectric properties and energy storage performances in Na_2O–BaO–PbO–Nb_2O_5–SiO_2–Al_2O_3 glass–ceramics. Ceram. Int. **44**, 23109–23115 (2018)
26. M.K. Prashant, T. Sankarappa, B.K. Vijaya, N. Nagaraja, Dielectric relaxation studies in transition metal ions doped tellurite glasses. Solid States Sci. **11**, 214–218 (2009)
27. M.K. Prashant, T. Sankarappa, K. Santhosh, AC conductivity studies in rare earth ions doped vanadotellurite glasses. J. Alloy Compd. **464**, 393–398 (2008)